Cellular Microbiology (2016) **18**(2), 244–259
doi:10.1111/cmi.12499
First published online 30 October 2015

The *Toxoplasma gondii* rhoptry protein ROP18 is an Irga6-specific kinase and regulated by the dense granule protein GRA7

Thomas Hermanns,[1] Urs B. Müller,[1] Stephanie Könen-Waisman,[1] Jonathan C. Howard[2] and Tobias Steinfeldt[1]*
[1]*Institute for Genetics, University of Cologne, Cologne, Germany.*
[2]*Fundação Calouste Gulbenkian, Instituto Gulbenkian de Ciência, Oeiras, Portugal.*

Summary

In mice, avirulent strains (e.g. types II and III) of the protozoan parasite *Toxoplasma gondii* are restricted by the immunity-related GTPase (IRG) resistance system. Loading of IRG proteins onto the parasitophorous vacuolar membrane (PVM) is required for vacuolar rupture resulting in parasite clearance. In virulent strain (e.g. type I) infections, polymorphic effector proteins ROP5 and ROP18 cooperate to phosphorylate and thereby inactivate mouse IRG proteins to preserve PVM integrity. In this study, we confirmed the dense granule protein GRA7 as an additional component of the ROP5/ROP18 kinase complex and identified GRA7 association with the PVM by direct binding to ROP5. The absence of GRA7 results in reduced phosphorylation of Irga6 correlated with increased vacuolar IRG protein amounts and attenuated virulence. Earlier work identified additional IRG proteins as targets of *T. gondii* ROP18 kinase. We show that the only specific target of ROP18 among IRG proteins is in fact Irga6. Similarly, we demonstrate that GRA7 is strictly an Irga6-specific virulence effector. This identifies *T. gondii* GRA7 as a regulator for ROP18-specific inactivation of Irga6. The structural diversity of the IRG proteins implies that certain family members constitute additional specific targets for other yet unknown *T. gondii* virulence effectors.

Received 9 May, 2015; revised 29 July, 2015; accepted 29 July, 2015. *For correspondence. E-mail tsteinfe@uni-koeln.de; Tel. (+49) 221 470 4868; Fax (+49) 221 470 6749.

Introduction

Hosts and pathogens impose intense selection pressures on each other, resulting in dynamic changes in the genetic structure of populations and rapid co-evolutionary change in molecules contributing to virulence and resistance. As JBS Haldane (1949) predicted, much polymorphic variation in protein sequence will arise from such interaction. A detailed analysis of polymorphic molecules involved in resistance and virulence provides insight into functional mechanisms, with potential implications for disease control. In this study, we analyse the biochemistry of an important polymorphic virulence complex secreted into mammalian cells by the ubiquitous protozoan pathogen *Toxoplasma gondii* (*T. gondii*).

T. gondii is an obligate intracellular parasite able to establish a productive infection in a remarkably broad range of mammalian and avian intermediate hosts, including man. Sexual reproduction occurs only in its primary host, i.e. all members of the family of true cats (*Felidae*). Because of their abundant worldwide distribution and sympatry with domestic cats, house mice are probably important intermediate hosts for *T. gondii* (Lilue *et al.*, 2013). Nevertheless, some strains of *T. gondii* are highly virulent for laboratory mice. Virulence in laboratory mice is associated with inactivation of the immunity-related GTPase (IRG) resistance system (Taylor, 2007; Taylor *et al.*, 2007). IRG proteins represent a complex family of polymorphic interferon gamma (IFNγ)-inducible GTPases (Boehm *et al.*, 1998; Martens and Howard, 2006). About 20 *IRG* genes are encoded within the genome of C57BL/6 mice, located in two adjacent clusters on chromosome 11 and one cluster on chromosome 18 (Bekpen *et al.*, 2005). Four of these genes are transcribed as adjacent pairs, resulting in expression of proteins carrying two IRG domains, the so-called tandem IRG proteins (Lilue *et al.*, 2013). Based upon a unique substitution within the first nucleotide binding motif (GX_4G**K**/**M**S), IRG proteins can be classified into two subfamilies. Activated GTP-bound effector IRG proteins (the G**K**S group) accumulate in high densities at the parasitophorous vacuolar membrane (PVM) of avirulent *T. gondii* type II strains early after invasion, leading to PVM rupture and parasite clearance (Martens *et al.*, 2005; Ling *et al.*, 2006; Zhao *et al.*, 2009b). The loading is cooperative

and hierarchical, with two family members serving as pioneers for members loading later (Khaminets *et al*., 2010). Premature activation of IRG effectors on cellular endomembranes is prevented by three regulatory IRG proteins, Irgm1–Irgm3 (the G**M**S group), which keep the effector proteins in a GDP-bound inactive conformation at endogenous cellular membranes (Hunn *et al*., 2008; Haldar *et al*., 2013; Maric-Biresev *et al*., in preparation). Exactly how IRG proteins contribute to disruption of the PVM is not known, but their essential, non-redundant function in early resistance of mice to avirulent *T. gondii* type II strains has been unambiguously established (Taylor *et al*., 2000; Collazo *et al*., 2001; Liesenfeld *et al*., 2011).

With *T. gondii* virulent type I strains, the initial loading of the PVM with IRG proteins is markedly reduced (Zhao *et al*., 2009c; Khaminets *et al*., 2010). In order to preserve the integrity of the PVM, *T. gondii* has evolved several polymorphic effector proteins (Hunter and Sibley, 2012; Alaganan *et al*., 2014; Etheridge *et al*., 2014). Genetic screens revealed that polymorphism in effectors accounts for the differences in virulence between *T. gondii* strains in infected mice (Saeij *et al*., 2006; Taylor *et al*., 2006; Saeij *et al*., 2007; Behnke *et al*., 2011). Different polymorphic rhoptry proteins were shown to be important for inhibition of the IRG resistance system. The catalytically active kinase ROP18 of *T. gondii* virulent type I strains phosphorylates IRG proteins at highly conserved threonines in the switch I region of the nucleotide binding site (Fentress *et al*., 2010; Steinfeldt *et al*., 2010). Phosphorylation of multiple family members could be demonstrated, but the target sites identified in Irga6 most closely match the ROP18 substrate phosphorylation motif (Lim *et al*., 2013). Certain *T. gondii* avirulent type II strains also express a virulent allelic form of ROP18 (Saeij *et al*., 2006; Niedelman *et al*., 2012) but fail to restrict IRG protein accumulation at the PVM to an extent that allows survival in infected mouse cells (Zhao *et al*., 2009b). We could demonstrate that for efficient phosphorylation, IRG proteins have to be kept in the inactive GDP-bound conformation (Fleckenstein *et al*., 2012). This conformation is facilitated by direct binding of the pseudokinase ROP5 to IRG proteins (Fleckenstein *et al*., 2012; Niedelman *et al*., 2012). Although not apparent for an IRG-specific function of ROP5 in our own experiments (Fleckenstein *et al*., 2012), an interaction of ROP5 with ROP18 was reported to control *T. gondii* virulence by up-regulation of ROP18 activity (Behnke *et al*., 2012). The *rop5* locus is represented by a cluster of tandemly repeated genes encoding three different ROP5 isoforms, ROP5A, ROP5B and ROP5C, each containing multiple copies, and all isoforms are predicted to be catalytically inactive (El Hajj *et al*., 2006; Reese and Boothroyd, 2011). Individual sequences of these *rop5* paralogues are almost identical within strains but differ considerably between *T. gondii* types I, II and III strains (Behnke *et al*., 2011; Reese *et al*., 2011; Niedelman *et al*., 2012). In wild-derived mice, this two-component ROP5/ROP18 parasite virulence system is counteracted by polymorphic tandem IRG proteins (Lilue *et al*., 2013), most likely due to active decoying of ROP5 and ROP18 leaving Irga6 unphosphorylated. Another active rhoptry kinase, ROP17, was demonstrated only recently to phosphorylate Irga6 and Irgb6 *in vitro*. ROP17 shows a preference for Irgb6, and unlike ROP18, kinase activity is independent from ROP5 (Etheridge *et al*., 2014).

In this study, we show that the dense granule protein GRA7 (Bonhomme *et al*., 1998; Fischer *et al*., 1998) is directly associated with ROP5 and is essential for efficient phosphorylation of Irga6. Consequently, the loss of GRA7 can be correlated directly with parasite virulence *in vitro* and *in vivo*. We conclusively demonstrate that GRA7 is an Irga6-specific *T. gondii* effector and propose a model explaining the molecular function of GRA7 by regulation of ROP18 kinase activity. This model is supported by our finding that Irga6 is also the only specific target of ROP18 among IRG proteins. Clarification of this Irga6-specific function of ROP18 *in vivo* suggests that other yet unknown *T. gondii* virulence effectors may be strictly specific for other IRG proteins.

Results

GRA7 is a component of the IRG-targeting ROP5/ROP18 kinase complex

In pull-down experiments from detergent lysates of L929 fibroblasts infected with virulent RH-YFP type I strain tachyzoites, several *T. gondii* proteins could be identified by liquid chromatography–tandem mass spectrometry (LC-MS/MS) to interact with glutathione S-transferase (GST)-Irga6 (Fleckenstein *et al*., 2012; Howard and Steinfeldt, unpublished results). To find which of these proteins might represent IRG-related *T. gondii* effector proteins, we first determined the composition of Irga6-specific complexes under non-denaturating conditions. After separation by blue native (BN) polyacrylamide gel electrophoresis (PAGE), LC-MS/MS analysis from similar pull-down experiments revealed that some of these proteins are indeed components of the same complex (Table S1). In addition to all ROP5 isoforms and ROP18, tryptic peptides were identified unambiguously corresponding to the dense granule protein GRA7. However, GRA7 was not found in pull-down approaches using detergent lysates of *T. gondii* RHΔ*rop5* strain. This result suggests ROP5 is required in an Irga6/GRA7 complex. The LC-MS/MS results obtained after BN-PAGE were confirmed by Western blot analysis (Fig. 1). ROP5 binding to Irga6 was unchanged in the absence of GRA7

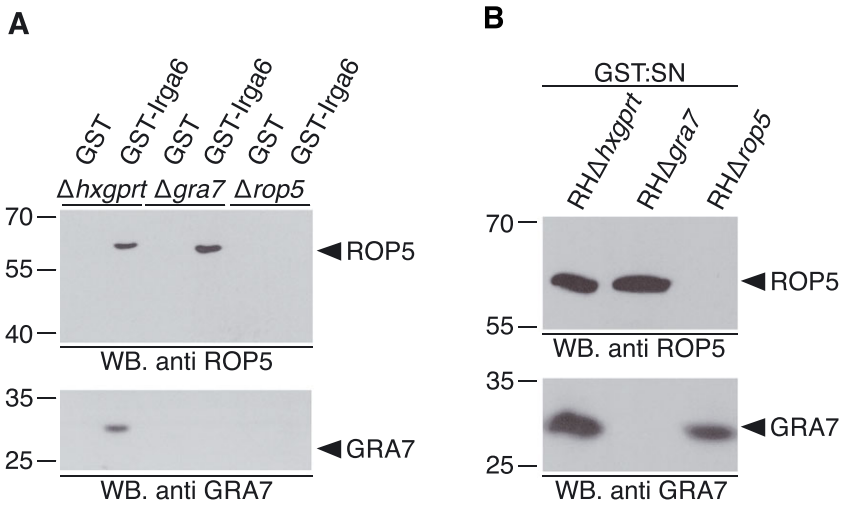

Fig. 1. GRA7 is recruited to the *Toxoplasma gondii* ROP5/ROP18 kinase complex via ROP5. *In vitro* pull-down with recombinant GST-Irga6 fusion protein or GST alone and *T. gondii* tachyzoite detergent lysates.
A. Pull-down of GRA7 (lower panel) by Irga6 from RHΔ*hxgprt* is completely lost in the absence of ROP5 expression (RHΔ*rop5*), RHΔ*gra7* served as control to confirm protein identity. Pull-down of ROP5 (upper panel) by Irga6 from RHΔ*hxgprt* and RHΔ*gra7*, RHΔ*rop5* served as control to confirm protein identity.
B. ROP5 (upper panel) and GRA7 (lower panel) levels in the supernatants from pull-downs with GST alone.

(RHΔ*gra7*), but no GRA7 could be detected when RHΔ*rop5* parasites were applied in the same pull-down approach. In parallel, GST alone was used and provided control for specificity (Fig. 1A). Equal protein amounts in tachyzoite lysates were confirmed in the supernatants after pull-down with GST (Fig. 1B).

The results shown in Fig. 1 indicate either that the interaction between Irga6 and GRA7 is indirect and mediated by ROP5 or that direct binding of GRA7 to Irga6 requires a conformational change of the GTPase induced by direct binding of ROP5 (Fleckenstein *et al.*, 2012).

GRA7 is directly associated with ROP5

We directly looked for GRA7 binding to ROP5, which we immunoprecipitated using a GRA7-specific antibody from *T. gondii* tachyzoite lysates or lysates of infected L929 cells that were stimulated with IFNγ or left untreated. Subsequent Western blot analysis using a ROP5-specific antibody revealed interaction of the parasite proteins in both tachyzoite lysates (Fig. 2A) and lysates from infected cells (Fig. 2B). In the latter case, prestimulation with IFNγ (middle panel) had no clearly visible effect on the intensity of GRA7 binding to ROP5. The impact of ROP5 on vacuolar GRA7 accumulation was investigated by signal intensity measurements at the PVM. In mouse embryonic fibroblasts (MEFs) stimulated with IFNγ and subsequently infected with *T. gondii*, the mean signal intensities of GRA7 were clearly decreased at RHΔ*rop5*-derived vacuoles compared with RHΔ*hxgprt* (Fig. 2C), indicating that association of a significant proportion of GRA7 with the *T. gondii* PVM is dependent on ROP5 in infected cells.

In summary, these results demonstrate that recruitment of GRA7 to the *T. gondii* kinase complex is dependent on binding to ROP5 but does not necessarily indicate a direct binary interaction.

In a yeast two-hybrid assay, *T. gondii* proteins GRA7 and ROP5A/B/C were expressed as N-terminal fusions with the Gal4 DNA-binding or Gal4 activation domain in a yeast reporter strain. Colony growth on selective medium allowed us to screen for direct protein–protein interactions. In this way, direct binding of GRA7 to all three ROP5 isoforms could be shown. No colony growth was observed for the negative controls (Fig. 2D).

GRA7 does not contribute to Irga6/ROP5/ROP18 complex assembly

In the following analysis, the presence of GRA7 as a basic requirement for the association of different complex members was investigated. Our pull-down results already demonstrated no differences in ROP5 binding to Irga6 in the presence or absence of *T. gondii* GRA7 expression (Fig. 1). Stimulation of ROP18 kinase activity was suggested earlier to be an important molecular function of ROP5 (Behnke *et al.*, 2012). We analysed ROP5 immunoprecipitations from detergent tachyzoite lysates of different *T. gondii* strains for binding of ROP18. Western blot analysis with a ROP18-specific antiserum demonstrated binding of ROP5 to ROP18 in *T. gondii* RHΔ*hxgprt* and RHΔ*gra7* detergent lysates (Fig. 3A, left-hand panel). No difference in binding of ROP5 to ROP18 in the absence of GRA7 was observed. Equal protein amounts in tachyzoite detergent lysates were confirmed in the supernatants after immunoprecipitation (Fig. 3A, right-hand panel). These results indicate that GRA7 is probably

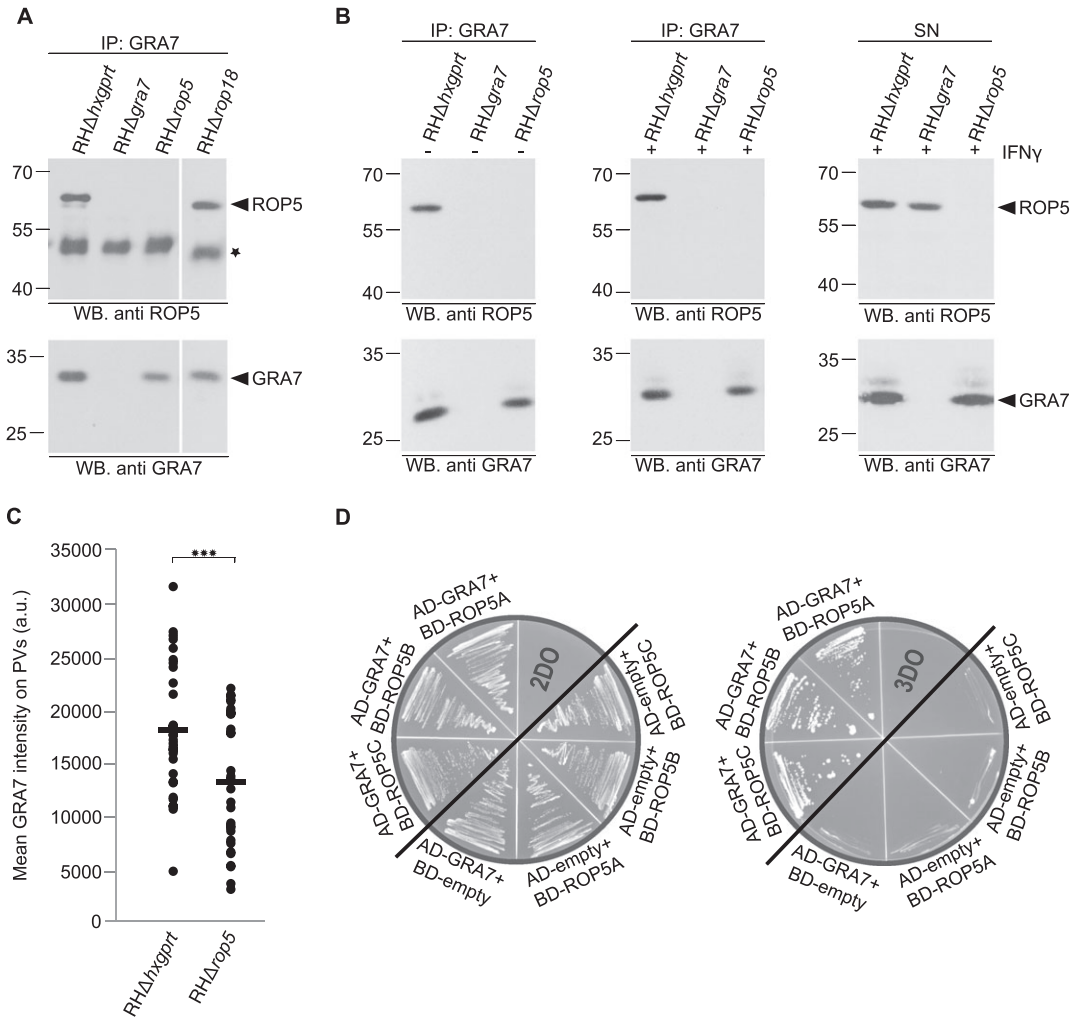

Fig. 2. GRA7 directly binds ROP5.
A. ROP5 co-immunoprecipitation (upper panel) from *Toxoplasma gondii* tachyzoite detergent lysates using 3.1.2 GRA7-specific monoclonal antibody (lower panel). Asterisk indicates heavy chain of the antibody used for immunoprecipitation. The white space indicates excision of irrelevant tracks.
B. ROP5 co-immunoprecipitation from *T. gondii*-infected L929 cells non-induced (left-hand panel) or induced with 200 U ml^{-1} of IFNγ (middle panel) using 3.1.2 GRA7-specific monoclonal antibody. The right-hand panel indicates ROP5 (upper panel) and GRA7 (lower panel) levels in the supernatants after immunoprecipitation.
C. GRA7 protein intensities are reduced at RHΔ*rop5*-derived vacuoles. IFNγ-induced MEFs (200 U ml^{-1}) were infected for 2 h with *T. gondii* RHΔ*hxgprt* or RHΔ*rop5* and individual GRA7 protein-positive vacuoles identified with 2.4.21 monoclonal antibody. One representative out of two independent experiments is shown (30 vacuoles counted).
D. GRA7 directly interacts with all ROP5 isoforms in a yeast two-hybrid approach. Cotransformants grown on double-dropout (2DO) plates were replica-plated under 2DO (SD/-Leu/-Trp) and triple-dropout (3DO, SD/-Leu/-Trp/-His) conditions. Colony growth under 3DO conditions is indicative of a GRA7:ROP5 interaction. Grey lines separate samples from the negative controls. Note that the negative controls plated on 3DO plates show remains of spotted material that does not represent colony growth.

not required for the association of the ROP5/ROP18 complex.

Interestingly, after immunoprecipitation of GRA7 from *T. gondii* detergent lysates, Western blot analysis with a ROP18-specific antiserum revealed interaction of ROP18 with GRA7 only in the absence of ROP5 (Fig. 3B, upper panel). Efficiency of immunoprecipitation (GRA7) in the case of RHΔ*hxgprt* and RHΔ*rop5* is indicated (Fig. 3B, lower panel). To investigate a direct interaction of GRA7 and ROP18, proteins were expressed as N-terminal fusions with the Gal4 DNA-binding (ROP18) or Gal4 activation domain (GRA7) in a yeast reporter strain. Direct binding of GRA7 to ROP18 is indicated by colony growth on selective medium compared with the negative controls (Fig. 3C).

GRA7 is required for efficient phosphorylation of Irga6

The association of GRA7 with ROP5 (Fig. 2) and ROP18 (Fig. 3) indicated that GRA7 is a component of

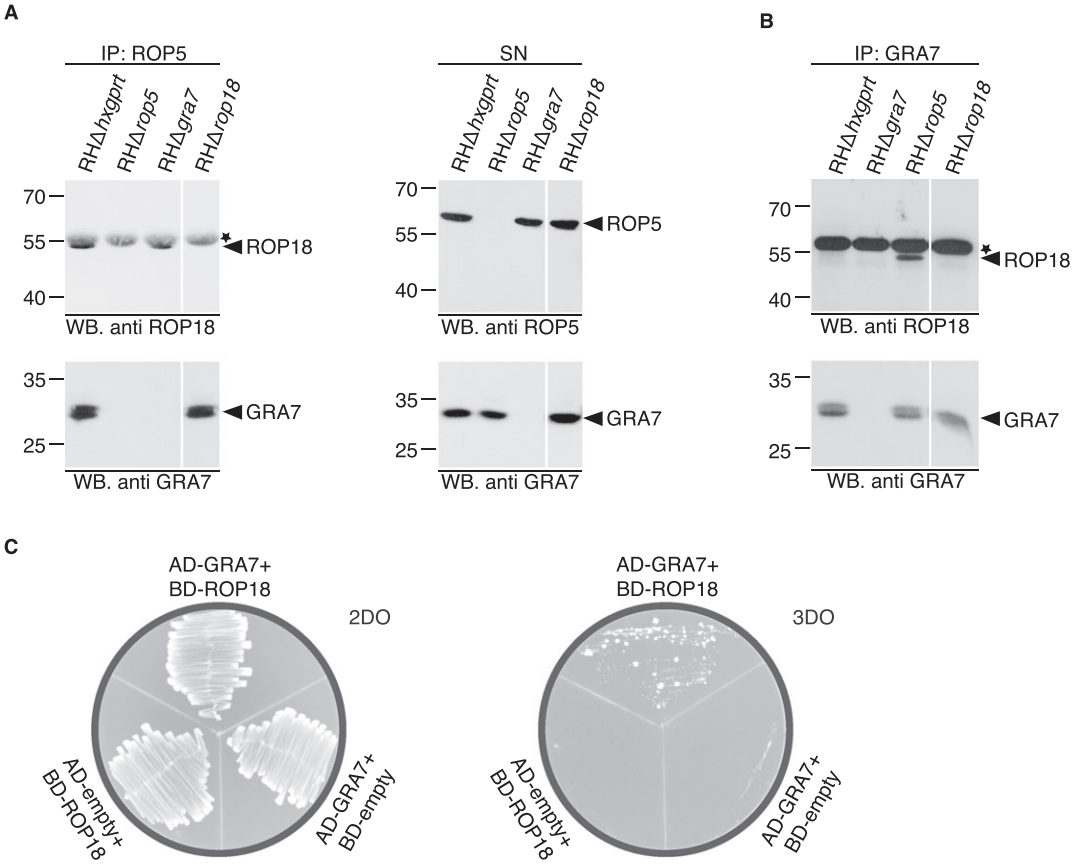

Fig. 3. GRA7 and ROP5 interact with ROP18.
A. ROP18 co-immunoprecipitates with ROP5 from *T. gondii* tachyzoite detergent lysates. Co-immunoprecipitation of ROP18 with ROP5 (upper panel) from RHΔ*hxgprt* and RHΔ*gra7* using 3E2 ROP5-specific monoclonal antibody. The lower panel indicates equivalent co-immunoprecipitation of GRA7 from RHΔ*hxgprt* and RHΔ*rop18*. The right-hand blot indicates ROP5 (upper panel) and GRA7 (lower panel) levels in the supernatants after immunoprecipitation.
B. ROP18 co-immunoprecipitates with GRA7 from *T. gondii* tachyzoite detergent lysates. Co-immunoprecipitation of ROP18 with GRA7 (upper panel) is only visible from RHΔ*rop5* but not RHΔ*hxgprt*, RHΔ*gra7* or RHΔ*rop18* using 3.1.2 GRA7-specific monoclonal antibody. The lower panel indicates equivalent levels of GRA7 in the immunoprecipitations. Asterisks indicate heavy chain of the respective antibody used for immunoprecipitation. White spaces indicate excision of irrelevant tracks.
C. GRA7 and ROP18 directly interact in a yeast two-hybrid approach. Cotransformants grown on double-dropout (2DO) plates were replica-plated under 2DO (SD/-Leu/-Trp) and triple-dropout (3DO, SD/-Leu/-Trp/-His) conditions. Colony growth under 3DO conditions is indicative of a GRA7 : ROP18 interaction.

the *T. gondii* kinase complex. In the following, we were able to demonstrate that GRA7 indeed contributes to phosphorylation and inactivation of the IRG resistance system.

MEFs stimulated with IFNγ for 24 h were infected with *T. gondii* RHΔ*hxgprt*, RHΔ*rop5* or RHΔ*gra7* strain for a further 2 h. Western blot analysis of detergent lysates indicated diminished phosphorylation of Irga6 at T108 [(pT108)Irga6], one of the ROP18 target threonines, in the absence of GRA7 expression compared with parental strain-infected cells. As expected, no phosphorylation was detectable in the absence of ROP5 (Fig. 4A, right-hand panel). ROP5 and GRA7 expression levels in the lysates of infected cells served as infection control (Fig. 4A, left-hand panels), and calnexin (Fig. 4A, upper panels) provided loading controls. Expression levels of ROP18 and ROP5 were comparable in RHΔ*hxgprt* and RHΔ*gra7* tachyzoite detergent lysates (Fig. S1).

The reduced phosphorylation of Irga6 in RHΔ*gra7* strain-infected cells seen in Western blot was confirmed by fluorescence signal intensity measurements at individual vacuoles in MEFs 2 h post-infection. Compared with parental strain-infected cells, mean signal intensities of (pT108)Irga6 were significantly decreased in RHΔ*gra7*-infected MEFs (Fig. 4B). These results clearly indicate that GRA7 is an important component within the *T. gondii* kinase complex, contributing to phosphorylation of Irga6 by ROP5 and ROP18 (Fentress *et al.*, 2010; Steinfeldt *et al.*, 2010; Fleckenstein *et al.*, 2012).

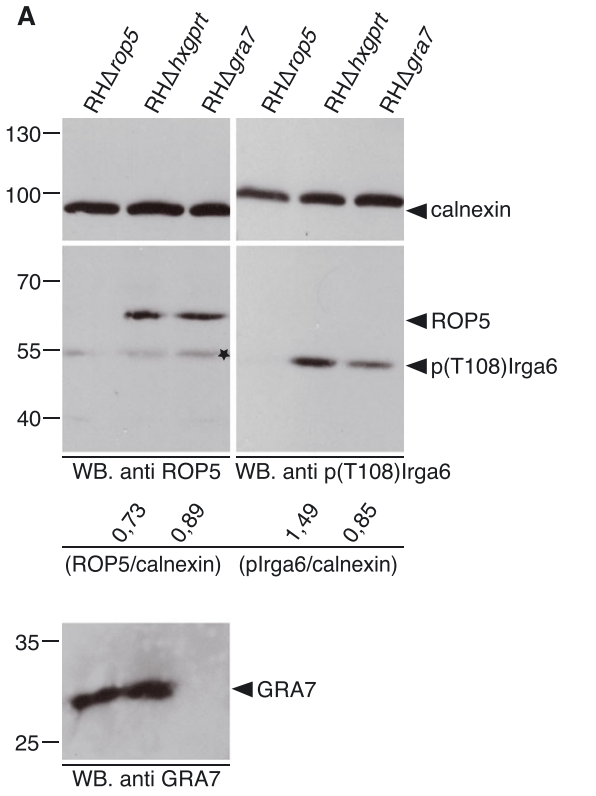

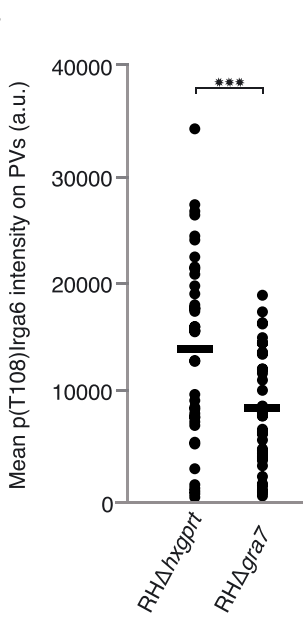

Fig. 4. *Toxoplasma gondii*-derived GRA7 is important for efficient Irga6 phosphorylation.
A. Western blot of detergent lysates from C57BL/6 MEFs stimulated for 24 h with 200 U ml^{-1} of IFNγ and infected for 2 h with *T. gondii* RHΔ*rop5*, RHΔ*hxgprt* or RHΔ*gra7*. The signal representing phosphorylation of Irga6 at T108 [p(T108)Irga6] upon RHΔ*hxgprt* infection is clearly reduced upon infection with RHΔ*gra7* (middle right panel). Signals for ROP5 (middle left panel) and GRA7 (lower panel) indicate equivalent levels of infection. Band intensities relative to calnexin were determined using ImageJ software. Asterisk indicates unspecific proteins. Calnexin (upper panels) served as loading control.
B. In MEFs, induced for 24 h with 200 U ml^{-1} of IFNγ and infected for 2 h with *T. gondii* RHΔ*hxgprt* or RHΔ*gra7*, signal intensities of p(T108)Irga6 at the PVM were determined using anti-p(T108)Irga6-specific antibody. One representative out of two independent experiments is shown (40 vacuoles counted).

GRA7 contributes to inhibition of vacuolar IRG protein accumulation

With *T. gondii* virulent type I strains, IRG protein accumulation at the PVM is markedly reduced compared with type II or III avirulent strains (Zhao *et al.*, 2009a; 2009c; Khaminets *et al.*, 2010). The lack of efficient Irga6 phosphorylation by *T. gondii* RHΔ*gra7* (Fig. 4) predicted increased IRG protein amounts at the PVM relative to RHΔ*hxgprt*. We therefore determined recruitment of certain IRG proteins to the PVM in MEFs 2 h post-infection. Compared with RHΔ*hxgprt*, signal intensities (Figs 5A, B and S2) and frequencies of loaded vacuoles (Fig. S2) of Irga6, Irgb6, Irgb10 and Irgd were significantly increased in RHΔ*gra7*-infected cells.

Growth restriction of *T. gondii* by IFNγ in infected cells (Zhao *et al.*, 2009b) is directly associated with inhibition of efficient IRG protein loading onto the PVM. We measured intracellular proliferation of *T. gondii* RHΔ*gra7* in bone marrow-derived macrophages (BMMs) and MEFs *in vitro* by incorporation of ^{3}H-uracil. The inability of RHΔ*gra7* parasites to prevent IRG protein accumulation at the PVM (Figs 5A, B and S2) was reflected in significantly greater inhibition of intracellular replication relative to *T. gondii* RHΔ*hxgprt* upon stimulation with IFNγ (Fig. 5C). Therefore, the impact of GRA7 on IRG protein accumulation is directly correlated with control of parasite replication in cells *in vitro*.

We next investigated the contribution of GRA7 to *T. gondii* virulence in mice. The virulence difference between RHΔ*hxgprt* and RHΔ*gra7* cannot be resolved in C57BL/6 mice (Alaganan *et al.*, 2014) (Fig. 6D). However, the wild-derived Indian mouse strain CIM is considerably more resistant to type I *T. gondii* strains (Lilue *et al.*, 2013). The median lethal dose of RHΔ*hxgprt* injected intraperitoneally in these mice was determined to be between 1×10^{5} and 1×10^{6} parasites (Fig. S3). Almost all CIM mice infected with 5×10^{5} RHΔ*hxgprt* tachyzoites died within 25 days post-infection, whereas in RHΔ*gra7* and RHΔ*rop18* infections, time to death was slightly delayed and more mice survived the infection (Fig. 5D). Slightly reduced virulence of RHΔ*gra7* was also reported by Alaganan *et al.* (2014) in CD-1 mice.

The impact of GRA7 on IRG protein accumulation is Irga6-specific

Among all IRG-related *T. gondii* effectors identified so far, ROP5 had the largest effect on vacuolar IRG protein accumulation. We therefore wanted to compare the impact of GRA7 with ROP5. Whereas signal intensities of Irgb6 and Irgb10 at RHΔ*gra7*-derived vacuoles were found to be intermediate between vacuoles derived from RHΔ*rop5* and RHΔ*hxgprt*, the vacuolar loading phenotype of Irga6

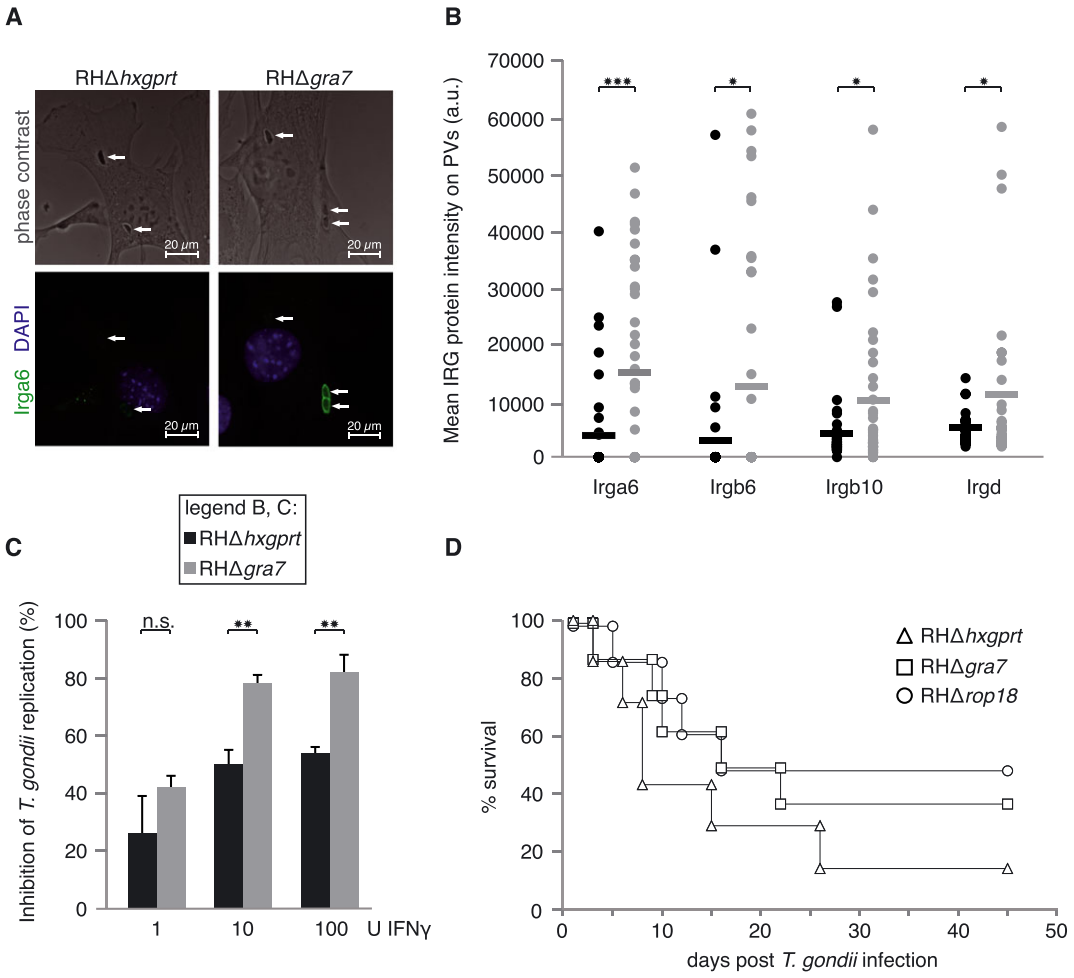

Fig. 5. GRA7 is necessary for parasite control *in vitro* and *in vivo*. (A, B) IFNγ-induced (200 U ml^{-1}) MEFs were infected for 2 h with *T. gondii* RHΔ*hxgprt* or RHΔ*gra7* and individual IRG proteins identified with mouse monoclonal antibody 10D7 (Irga6) and B34 (Irgb6) or 940/6 (Irgb10) and 2078 (Irgd) rabbit antisera.

A. Upper panels: phase contrast images. Lower panels: fluorescent images of vacuoles (white arrows) from RHΔ*hxgprt*-infected or RHΔ*gra7*-infected MEFs. Irga6 (green), nuclei stained with 4′,6-diamidino-2-phenylindole (blue).

B. The fluorescent signal intensities of each IRG protein were determined on coded slides in at least two independent experiments. One representative experiment is shown, and horizontal lines indicate means (30–35 vacuoles counted).

C. C57BL/6 BMMs were induced with 1, 10 or 100 U ml^{-1} of IFNγ for 24 h and infected with *T. gondii* RHΔ*hxgprt* or RHΔ*gra7* at an MOI of 0.3. Intracellular parasite growth was calculated by incorporation of ^{3}H-uracil 24 h post-infection as described in *Experimental procedures*. The percentages are averages of triplicates, and the error bar represents the standard deviation for these averages.

D. CIM mice were infected by intraperitoneal injection of 5×10^{5} *T. gondii* RHΔ*hxgprt* ($n = 7$), RHΔ*gra7* or RHΔ*rop18* ($n = 8$) strain tachyzoites, and survival was monitored for 45 days.

was very similar in RHΔ*gra7*-infected and RHΔ*rop5*-infected cells (Fig. 6A). Based on the fact that GRA7 is directly associated with ROP5 (Fig. 2), RHΔ*rop5* is a functional RHΔ*rop5*/*gra7* strain in terms of Irga6 phosphorylation. Because the impact of single (RHΔ*gra7*) and functional double knockout (ko) mutant (RHΔ*rop5*/*gra7*) on Irga6 but not Irgb6 or Irgb10 loading is exactly the same, these results suggested an Irga6-specific function of GRA7.

To confirm an Irga6-specific function of GRA7, fluorescence signal intensities of Irgb6 and Irgb10 at the PVM were determined in *Irga6* ko MEFs. No difference in the mean total protein amounts of either Irgb6 or Irgb10 could be observed in these cells infected with *T. gondii* RHΔ*gra7* strain in comparison with RHΔ*hxgprt*. Both strains displayed a virulent phenotype as defined by IRG protein loading at the PVM (Fig. 6B). The vacuolar Irgb6 and Irgb10 accumulation at RHΔ*rop5*-derived vacuoles on the other hand was only slightly inhibited in *Irga6* ko MEFs (Fig. 6B). Equal IRG protein expression levels in wild type (wt) and ko cells were confirmed by Western blot analysis from detergent lysates of MEFs stimulated with IFNγ (Fig. S4). These observations show an Irga6-specific effect of *T. gondii* dense granule protein GRA7. Increased

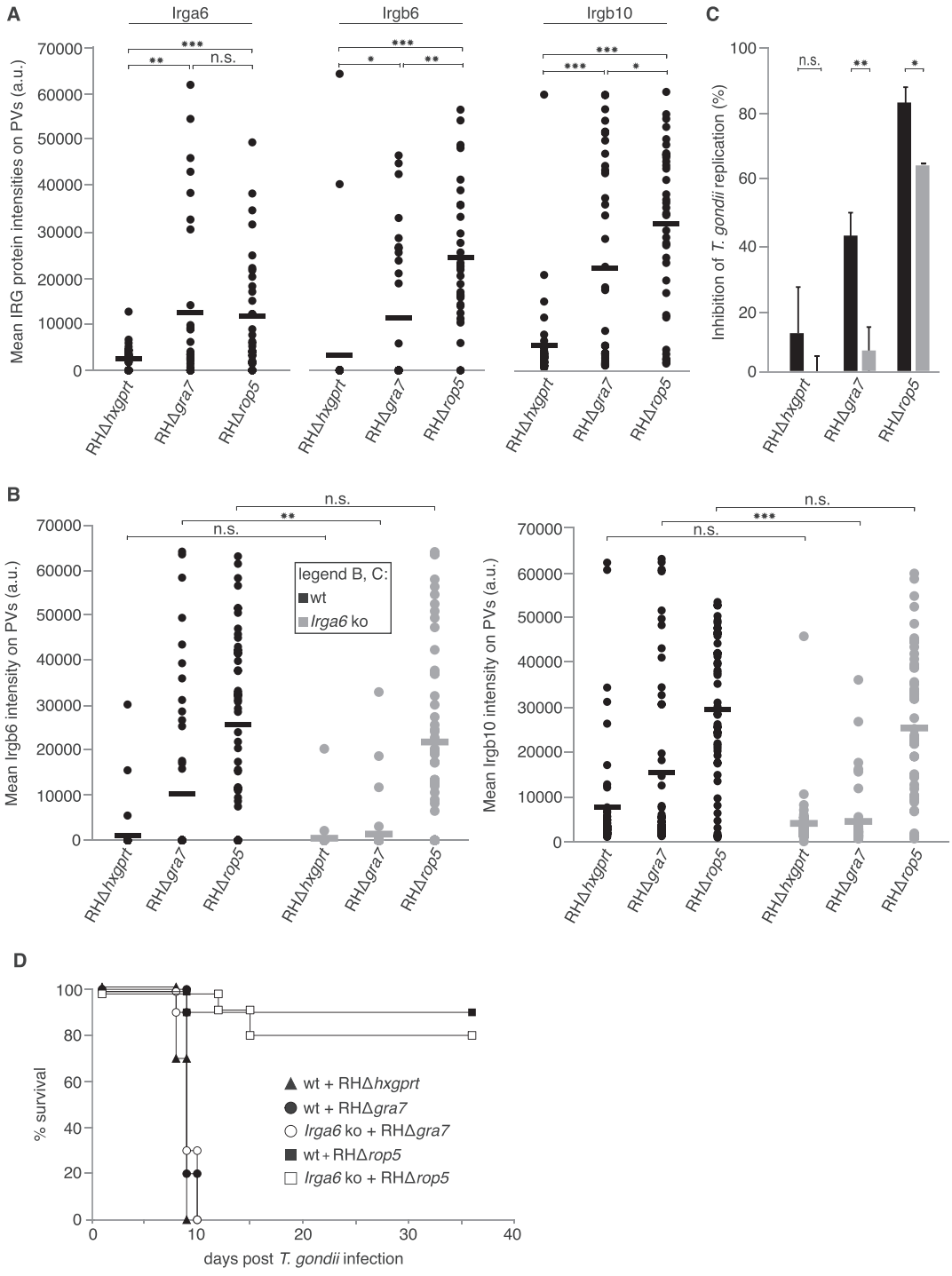

Fig. 6. GRA7 is an Irga6-specific *T. gondii* virulence effector.
A. IFNγ-induced (200 U ml^{-1}) wt MEFs were infected for 2 h with *T. gondii* RHΔ*hxgprt*, RHΔ*rop5* or RHΔ*gra7* and individual IRG protein positive vacuoles evaluated, 30 vacuoles counted. One representative out of two independent experiments is shown.
B. IFNγ-induced (200 U ml^{-1}) wt or *Irga6* ko MEFs were infected for 2 h with *T. gondii* RHΔ*hxgprt*, RHΔ*rop5* or RHΔ*gra7* and individual IRG protein positive vacuoles evaluated, 50 vacuoles counted. One representative out of two independent experiments is shown.
C. wt and *Irga6* ko MEFs were induced with 10 U ml^{-1} of IFNγ for 24 h and infected with *T. gondii* RHΔ*hxgprt*, RHΔ*gra7* or RHΔ*rop5* at an MOI of 1.
D. Virulence of *T. gondii* RHΔ*hxgprt*, RHΔ*gra7* and RHΔ*rop5* in wt and *Irga6* ko mice. C57BL/6 wt (n = 10) and *Irga6* ko (n = 10) mice were infected by intraperitoneal injection of 50 *T. gondii* RHΔ*hxgprt*, RHΔ*gra7* or 200 RHΔ*rop5* strain parasites and survival monitored for 36 days.

amounts of Irgb6 and Irgb10 at RHΔ*gra7*-derived vacuoles in wt MEFs (Fig. 6A) are dependent only on elevated levels of Irga6, a cooperative interaction documented earlier (Khaminets *et al*., 2010).

The Irga6 specificity of *T. gondii* GRA7 was confirmed by intracellular proliferation in *Irga6* ko MEFs. In contrast to its attenuated virulence phenotype in wt cells (Figs. 6C, and 5C), proliferation in *Irga6* ko MEFs (Fig. 6C) was not efficiently restricted by IFNγ, and *T. gondii* RHΔ*gra7* almost behaved like virulent RHΔ*hxgprt* in these cells. According to its vacuolar IRG protein loading phenotype (Fig. 6B), proliferation of RHΔ*rop5* was still strikingly inhibited in the presence of IFNγ in *Irga6* ko MEFs (Fig. 6C). We next investigated *T. gondii* virulence *in vivo*. After challenge with RHΔ*gra7*, *Irga6* ko and wt mice succumbed to infection within ten days whereas almost all wt and ko mice challenged with RHΔ*rop5* parasites survived infection (Fig. 6D).

Irga6 is the main target of ROP18 among IRG proteins in BL/6 mice

The importance of GRA7 for full ROP18 kinase activity (Fig. 4) and its apparent specificity for Irga6 (Fig. 6) stimulated us to investigate whether the overall impact of ROP18 on the IRG resistance system (Fentress *et al*., 2010; Steinfeldt *et al*., 2010; Behnke *et al*., 2012; Fleckenstein *et al*., 2012; Niedelman *et al*., 2012) is also due only to specific inhibition of Irga6.

Fluorescence signal intensities and frequencies of loaded vacuoles of Irgb6 and Irgb10 were determined at the PVM in wt and *Irga6* ko MEFs 2 h post-infection with wt RHΔ*hxgprt* or RHΔ*rop18*. As shown earlier, Irgb6 and Irgb10 loading was substantially higher on RHΔ*rop18* than on wt vacuoles. However, the increase in loading intensity and number of positive vacuoles associated with loss of ROP18 was significantly diminished in *Irga6* ko cells (Figs 7A and S5). These results differ slightly from the complete extinction of Irgb6 and Irgb10 loading to RHΔ*gra7*-derived vacuoles in *Irga6* ko MEFs (Figs 7A, 6B and S5). In summary, these results indicate that the enhanced loading of Irgb6 and Irgb10 at the PVM in RHΔ*rop18*-infected wt MEFs is largely an indirect effect of increased Irga6 amounts. In contrast, deletion of ROP5 resulted only in a marginal decrease of intensities (Fig. 7A) and frequencies (Fig. S5) of Irgb6 and Irgb10 at the *T. gondii* PVM in *Irga6* ko cells relative to wt cells.

The pattern of vacuolar IRG protein accumulation is directly correlated with control of proliferation in infected cells upon stimulation with IFNγ (Zhao *et al*., 2009c). The avirulent phenotype of RHΔ*rop18* in infected wt MEFs was reversed to a virulent phenotype in *Irga6* ko cells and in this way very similar to RHΔ*gra7*, whereas proliferation of RHΔ*rop5* was still efficiently inhibited in the absence of Irga6 expression relative to wt cells (Fig. 7B).

The *Irga6* deficiency also affects virulence of *T. gondii* RHΔ*rop18 in vivo*. After challenge with RHΔ*rop18*, *Irga6* ko mice succumbed to infection within 10 days, whereas in wt mice, time to death was significantly delayed (Fig. 7C).

With respect to IRG protein inactivation, these results are consistent with ROP18 being an Irga6-specific kinase.

Discussion

Virulence of *T. gondii* in mice is adjusted by dozens of parasite proteins injected into the host cell cytosol at the onset and after host cell invasion (Hunter and Sibley, 2012; Bougdour *et al*., 2013; Braun *et al*., 2013; Alaganan *et al*., 2014; Etheridge *et al*., 2014). The rhoptry proteins ROP5 and ROP18 have been shown to inhibit the IRG resistance system by phosphorylation of highly conserved threonine residues in the switch I region of the nucleotide binding site (Fentress *et al*., 2010; Steinfeldt *et al*., 2010; Behnke *et al*., 2012; Fleckenstein *et al*., 2012; Niedelman *et al*., 2012). In this study, we could confirm that the dense granule protein GRA7 is an additional component of the *T. gondii* ROP5/ROP18 kinase complex (Alaganan *et al*., 2014). GRA7 is directly associated with ROP5 and required for efficient phosphorylation of Irga6. In a recent study, direct GRA7 : Irga6 association was observed with purified proteins *in vitro* in the presence of GTP (Alaganan *et al*., 2014). However, in our pull-down analyses, GRA7 binding to Irga6 was always dependent on ROP5 regardless of whether additional GTP was added (data not shown) or not. Moreover, at the PVM of *T. gondii* RHΔ*rop5* in IFNγ-stimulated MEFs, GRA7 intensities were significantly, although not completely, reduced (Fig. 2C). A fraction of GRA7 is associated with the vacuolar network of tubular membranes rather than the PVM (Bonhomme *et al*., 1998), and in addition, binding of GRA7 to ROP2 and ROP4 was shown (Dunn *et al*., 2008), perhaps explaining the only partial decrease of vacuolar GRA7 amounts in the absence of ROP5.

In addition to Irga6, also Irgb6 and Irgb10 have been shown to be phosphorylated upon infection with *T. gondii* virulent type I strains in cells of laboratory mice (Fentress *et al*., 2010; Steinfeldt *et al*., 2010; Behnke *et al*., 2012; Lilue *et al*., 2013), and inactivation by the ROP5/ROP18/GRA7 kinase complex is accompanied by reduced accumulation at the PVM (e.g. Fig. 7A). However, our data show that the effect of GRA7 and ROP18 on other IRG proteins is mediated through Irga6. Thus, attenuation of the kinase complex by loss of GRA7 (in RHΔ*gra7*) or ROP18 (in RHΔ*rop18*) caused significant increases in signals at the PVM of Irgb6, Irgb10 and Irgd in wt MEFs but had little or no effect on PVM accumulation in *Irga6* ko

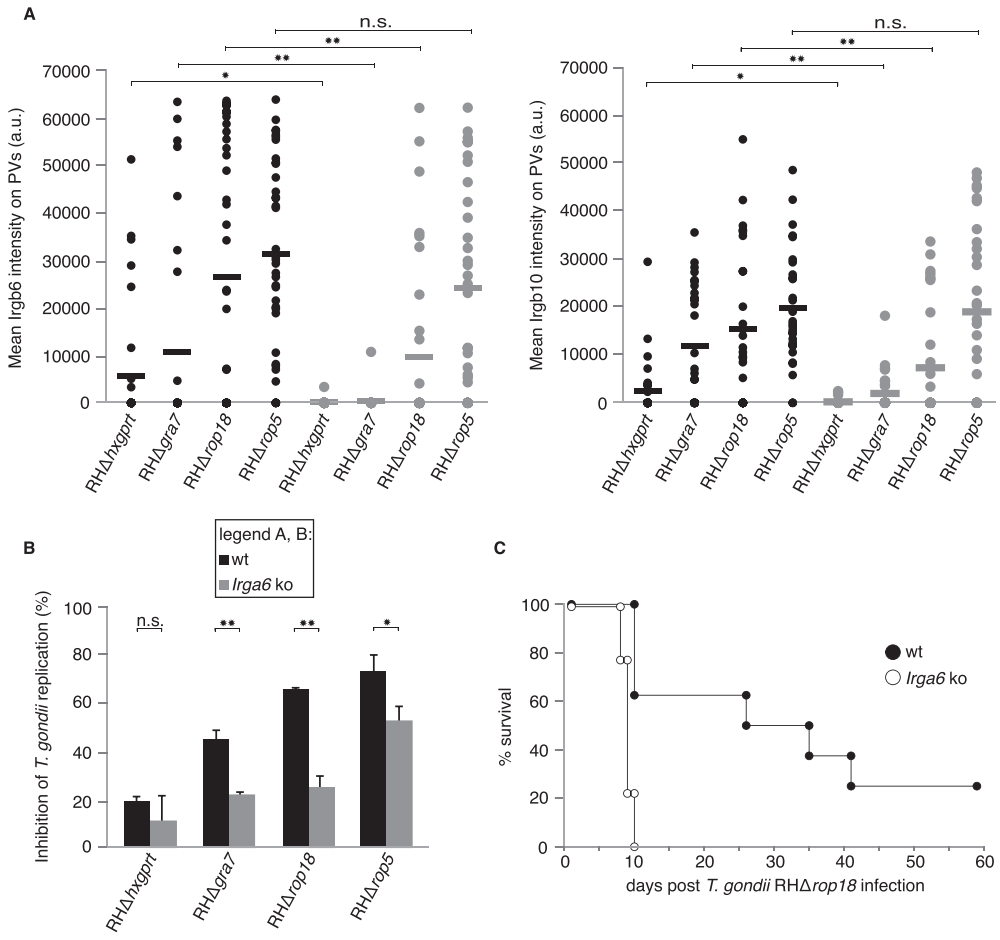

Fig. 7. Irga6 is the only specific target of ROP18 among IRG proteins.
A. After infection of IFNγ-induced (200 U ml^{-1}) wt or *Irga6* ko MEFs for 2 h with *Toxoplasma gondii* RHΔ*hxgprt*, RHΔ*gra7*, RHΔ*rop18* or RHΔ*rop5*, individual Irgb6 and Irgb10 protein positive vacuoles were analysed. One representative out of two independent experiments is shown (30 vacuoles counted).
B. wt and *Irga6* ko MEFs were induced with 10 U ml^{-1} IFNγ for 24 h and infected with *T. gondii* RHΔ*hxgprt*, RHΔ*gra7*, RHΔ*rop18* or RHΔ*rop5* at an MOI of 1.
C. Virulence of *T. gondii* RHΔ*rop18* in wt and *Irga6* ko mice. C57BL/6 wt ($n = 8$) and *Irga6* ko ($n = 9$) mice were infected by intraperitoneal injection of 200 *T. gondii* RHΔ*rop18* strain parasites, and survival was monitored for 60 days.

cells. Likewise, RHΔ*gra7* and RHΔ*rop18* were converted from parasite strains with an attenuated virulence phenotype in wt cells to fully virulent strains in *Irga6* ko cells (Figs 6 and 7). Strikingly and in contrast to RHΔ*rop5*, RHΔ*rop18* is fully virulent in *Irga6* ko mice (Figs 6D and 7C). These results illustrate the interdependent accumulation of IRG proteins at the *T. gondii* PVM documented earlier (Khaminets *et al*., 2010) and clearly demonstrate a molecular function of GRA7 and ROP18 that is specific for Irga6. The fact that loading of Irgb6 and Irgb10 in *Irga6* ko cells infected with RHΔ*rop18* is markedly lower than in the same cells infected with the completely avirulent RHΔ*rop5* shows again the existence of ROP5-dependent, ROP18-independent virulence actions against IRG proteins (Fleckenstein *et al*., 2012). ROP17 has recently been found to be a significant virulence factor targeting and phosphorylating Irgb6, but this action is reported to be independent of ROP5 (Etheridge *et al*., 2014). It is a challenge for future experiments to determine the precise mechanism of ROP5 in terms of Irgb6 and Irgb10 inactivation or to identify the proteins, in case they exist, necessary for its still unknown contribution to *T. gondii* virulence.

Although it is clear that GRA7 contributes to the ROP5/ROP18 kinase complex, loss of GRA7 does not attenuate RHΔ*hxgprt* virulence *in vivo* very much. After infection with *T. gondii* RHΔ*gra7*, C57BL/6 wt mice and *Irga6* ko mice died with identical kinetics as animals infected with wt parasites (Fig. 6D). Similarly, in a study published by Alaganan and colleagues, the authors showed a slightly attenuated virulence phenotype of RHΔ*gra7* in CD-1 outbred mice but not in C57BL/6

mice after infection with the same number of parasites. However, the double deletion mutant RHΔ*gra7*/Δ*rop18* had a completely avirulent phenotype in C57BL/6 wt mice (Alaganan *et al*., 2014). This result is unexpected, if both components contribute to virulence exclusively through Irga6 because resistance of C57BL/6 mice even to avirulent type II strains is only partially lost by deletion of *Irga6* (Liesenfeld *et al*., 2011). These seemingly paradoxical results are however consistent with the idea that Irga6 is a major player in resistance of laboratory mice against type I strain RHΔ*hxgprt* attenuated by loss of ROP18/GRA7 (Alaganan *et al*., 2014), while the residual resistance of *Irga6* ko laboratory mice to type II ME49 is largely mediated by other IRG proteins. However, virulence of single deletion mutants RHΔ*gra7* and RHΔ*rop18* is similarly attenuated relative to RHΔ*hxgprt* in the highly resistant CIM mouse strain (Fig. 5D), as expected if GRA7 function is required for full ROP18 kinase activity. The different virulence phenotypes of *T. gondii* RHΔ*gra7* in wild-derived mice (this study) and inbred and outbred laboratory strains of mice (this study and Alaganan *et al*., 2014) could be explained by genetic differences but need further investigation. Although no IFNγ-mediated control of *T. gondii* RHΔ*gra7* replication was observed previously (Alaganan *et al*., 2014), attenuated virulence of RHΔ*gra7* compared with wt infections could be well established in this study in bone marrow-derived macrophages (Fig. 5C) and fibroblasts (Figs 6C and 7B). These different observations might be explained by different cells or methods used to determine parasite replication.

No differences were observed in binding of ROP5 either to Irga6 or ROP18 in the absence of GRA7 (Figs 1 and 3A), indicating that the presence of GRA7 does not contribute significantly to the strength of the interaction between different members of the complex. Surprisingly, we were able to demonstrate GRA7 binding to ROP18 only in the absence of ROP5. It is conceivable that, in the presence of ROP5, the interface necessary for GRA7 : ROP18 interaction is either occupied or not fully accessible because of steric hindrances upon binding of ROP5. We also have to consider that our assay might not be sensitive enough to detect such an interaction in the presence of ROP5. Therefore, we cannot exclude at this point that direct binding of GRA7 is crucial for ROP18 activity even in the presence of ROP5. However, the whole scenario of IRG protein inactivation is played out at the PVM (Fentress *et al*., 2012). It is therefore possible that the interplay of certain components is indeed GRA7-dependent but could not be revealed in our *in vitro* systems. Furthermore, the existence of additional yet unidentified parasite proteins important for inactivation of Irga6 cannot be excluded.

The interaction between Irga6 and ROP5 has been crystallized from purified components (Reese *et al*., 2014) and does not require post-translational modification of either protein. Yet, both phosphorylation and glycosylation have been reported for members of the ROP5/ROP18/GRA7 complex (Dunn *et al*., 2008; Luo *et al*., 2011; Treeck *et al*., 2011). It is possible that some of these modifications may be involved in the interactions between components of the kinase complex. In a recent study, Lim *et al*. (2013) identified a potential ligand-binding pocket within the crystal structure of the ROP18 kinase domain adjacent to the active site and critical for ROP18-mediated virulence. The existence of this ligand-binding pocket, which contained a sucrose molecule derived from the crystallization buffer, might be indicative of co-translational or post-translational modification of GRA7 that could play a role in *T. gondii* virulence in general and ROP18 activation especially.

This study shows that GRA7 is a component of the *T. gondii* ROP5/ROP18 complex necessary to achieve efficient ROP18 kinase activity for the phosphorylation and consequent inactivation specifically of Irga6 (Fig. 8). Our results confirm Irga6 as an important target of *T. gondii* to promote parasite virulence. This is consistent with a former study that demonstrated a significant role for Irga6 in the control of *T. gondii* avirulent type II strain infection *in vivo* (Liesenfeld *et al*., 2011). By a specific attack on this highly conserved member (Lilue *et al*., 2013) of the family of IRG proteins, the complex pattern of IRG protein loading onto the *T. gondii* PVM is significantly disturbed and guarantees a growth advantage *in vitro* and *in vivo*. Just as Irga6 could be identified in this study as the only ROP18-specific target among IRG proteins, ROP17 has recently been found to be a significant virulence factor preferably phosphorylating Irgb6, but this action is reported to be independent of ROP5 (Etheridge *et al*., 2014). These findings strongly suggest that other *T. gondii* rhoptry effectors might have co-evolved to specifically inactivate other IRG proteins (Fig. 8). Future experiments will identify these genetic matches to better understand the inhibition of vacuolar IRG protein accumulation by virulent *T. gondii* strains to guarantee parasite survival in mice. These experiments document the intimacy and complexity of the co-evolving resistance–virulence contest played out between *T. gondii* and its mouse host. However, here we have considered only the interaction of one strain of *T. gondii* and its virulence mutants with the IRG proteins of the C57BL/6 strain of mouse. Yet the IRG proteins are themselves at least as polymorphic as the virulence factors that target them (Lilue *et al*., 2013), and how these structural variants contribute to adaptive outcomes for host and pathogen in the wild remains an important area for future research.

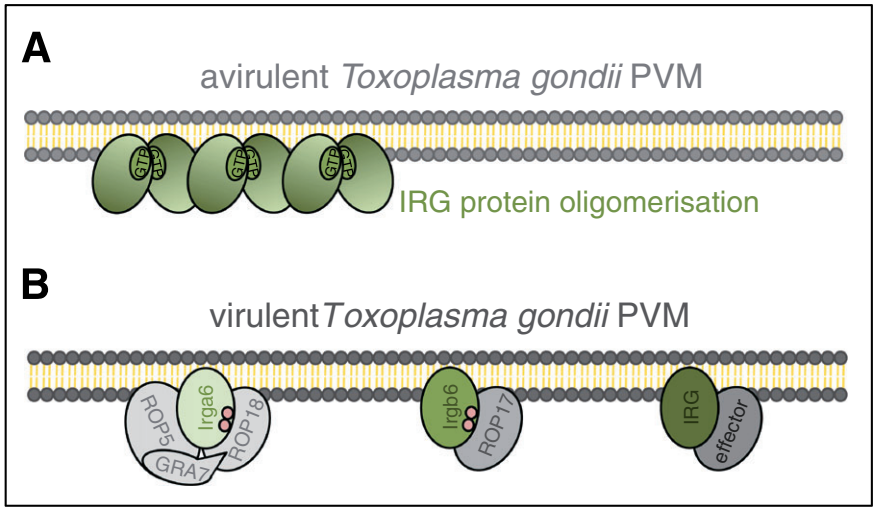

Fig. 8. Model for matched-genotype inhibition of IRG proteins by *Toxoplasma gondii* virulence effectors.
A. IRG protein oligomerization usually observed at the PVM of *T. gondii* avirulent strains (e.g. types II and III) is a prerequisite for its disruption and parasite clearance.
B. Virulent alleles of *T. gondii* pseudokinase ROP5 directly bind Irga6, holding it in a monomeric conformation and preventing formation of GTP-dependent Irga6 oligomers. Direct interaction of GRA7 with ROP5 is required for specific phosphorylation at two conserved threonine residues (red circles) and thereby permanent inactivation of Irga6 by ROP18, whereas ROP17 was shown to preferentially phosphorylate Irgb6 independent from ROP5 (Etheridge *et al.*, 2014). Other yet unknown *T. gondii* effectors have probably co-evolved to specifically inactivate other IRG proteins.

Experimental procedures

Propagation of T. gondii

Tachyzoites of *T. gondii* strains RHΔ*hxgprt*, RHΔ*gra7*, RHΔ*rop5* and RHΔ*rop18* were cultivated in confluent monolayers of human foreskin fibroblasts (HS27, ATCC CRL-1634), harvested and immediately used for infection of cells or lysed for subsequent immunoprecipitation, pull-down experiments or Western blot analysis.

Cell culture

L929 mouse fibroblasts and wt or *Irga6* ko MEFs derived from C57BL/6 mice were maintained by serial passage in Dulbecco's modified Eagle medium (DMEM), high glucose (Invitrogen Life Technologies) supplemented with 2 mM of L-glutamine, 1 mM of sodium pyruvate, 1× minimal essential medium non-essential amino acids, 100 U ml^{-1} of penicillin, 100 mg ml^{-1} of streptomycin (PAA) and 10% fetal calf serum (FCS, Biochrom). C57BL/6 BMMs were cultured in DMEM, high glucose containing 10% L929 P2 cell-conditioned medium and supplements indicated earlier. IRG protein expression was induced with 200 U ml^{-1} of IFNγ (Cell Concepts) for 24 h before infection. Human foreskin fibroblasts (HS27, ATCC CRL-1634) were maintained in Iscove's modified Dulbecco's medium, high glucose (Invitrogen Life Technologies) supplemented with 100 U ml^{-1} of penicillin, 100 mg ml^{-1} of streptomycin and 5% FCS.

Immunological reagents

Immunoreagents used in this study were 3E2 mouse monoclonal antibody against ROP5 isoforms (Leriche and Dubremetz, 1991), anti-ROP18 rat antiserum (El Hajj and Dubremetz, unpublished), affinity-purified rabbit sera 87558 against (pT108)Irga6 (Steinfeldt *et al.*, 2010), 10D7 and 10E7 mouse monoclonal antibodies (Papic *et al.*, 2008) or 165 rabbit antiserum (Martens *et al.*, 2004) against Irga6, B34 mouse monoclonal antibody (Carlow *et al.*, 1998) against Irgb6, 940/6 rabbit antiserum (unpublished) against Irgb10, 2078 rabbit antiserum (Martens *et al.*, 2004) against Irgd, 3.1.2 and 2.4.21 rat monoclonal antibodies against *T. gondii* GRA7 (unpublished), and rabbit anti-calnexin antiserum (Calbiochem).

Alexa 488-labelled and Alexa 555-labelled goat anti-rabbit, donkey anti-mouse and goat anti-rat fluorescent antisera (Molecular Probes), donkey anti-rabbit horseradish peroxidase (HRP, GE Healthcare), goat anti-rat HRP (Jackson Immuno Research Laboratories) and goat anti-mouse HRP (Pierce) polyclonal antibodies were used as secondary reagents.

Postnuclear lysate preparation from free tachyzoites and infected cells

25–50 × 10^6 free *T. gondii* tachyzoites or 2,5 × 10^6 MEFs seeded in 10 cm plates, stimulated with 200 U ml^{-1} IFNγ for 24 h, subsequently infected for 2 h with *T. gondii* at a multiplicity of infection (MOI) of 7 and washed threefold with PBS were lysed in 800 µl NP-40-lysis buffer [0,1 % NP-40, 150 mM NaCl, 20 mM Tris/HCl (pH 7,6), 5 mM MgCl2 supplemented with protease inhibitors (Roche)] for 2 h under constant rotation at 4°C. Postnuclear lysates were subjected to immunoprecipitation or pull-down analysis.

5 x 10^6 extracellular *T. gondii* tachyzoites or 4 x 10^5 MEFs seeded in 6 cm plates, stimulated with 200 U ml^{-1} IFNγ for 24 h, subsequently infected for 2 h with *T. gondii* at a MOI of 7 and washed once with PBS were lysed in 50 to 100 µl NP-40-lysis buffer (0,5 % NP-40) for 1 h on ice. Postnuclear lysates were boiled in sample buffer and subjected to SDS-PAGE and Western blot.

Immunoprecipitation and pull-down analysis

Postnuclear lysates were incubated with the indicated antibodies for 2 h at 4°C followed by an additional 1 h incubation with 100 µl of 1:1 (lysis buffer) bead suspension of protein A-sepharose (Amersham) resin or used in pull-down experiments as described earlier (Fleckenstein *et al.*, 2012). Beads were washed threefold with lysis buffer and either stored at −80°C or immediately boiled in sample buffer [80 mM of Tris/HCl (pH 6.8), 5 mM of EDTA,

4% SDS, 34% sucrose, 40 mM of dithiothreitol and 0.002% bromophenol blue] for 5 min at 95°C and subjected to SDS-PAGE and Western blot or BN-PAGE.

Toxoplasma gondii replication assay

T. gondii proliferation in infected MEFs or BMMs was determined by incorporation of ^{3}H-uracil as described earlier (Könen-Waisman and Howard, 2007; Liesenfeld *et al.*, 2011).

Mice virulence assay

Mice were infected intraperitoneally with 300 μl of PBS containing freshly harvested tachyzoites of indicated *T. gondii* strains. Survivors were sacrificed at the indicated days post-infection and tested for seroconversion using the Toxocell Latex Kit (Biokit, Barcelona, Spain).

Expression and purification of recombinant Irga6

Recombinant protein GST-Irga6 was expressed and purified as described previously (Fleckenstein *et al.*, 2012).

Immunocytochemistry

Fixation and staining of C57BL/6 MEFs grown on coverslips was performed as described earlier (Steinfeldt *et al.*, 2010), and microscopy and image analysis were performed blind on coded slides essentially according to Khaminets *et al.* (2010). Intracellular parasites were identified from phase contrast images or from the pattern of *T. gondii* GRA7 staining.

Yeast two-hybrid assay

Saccharomyces cerevisiae strain PJ69-4α was incubated with 1 μg of plasmid DNA (pGAD-C3 or pGBD-C3 containing the indicated genes) in transformation buffer (40% polyethylene glycol 3350, 0.2 M of LiAc, 0.5 mg ml^{-1} of single-stranded DNA and 0.1 M of dithiothreitol) for 30 min at 42°C. Cotransformants were selected by plating on double-dropout media (SD/-Leu/-Trp). Colonies grown on double-dropout media were replica-plated on triple-dropout media (SD/-Leu/-Trp/-His) containing 0.5 mM of 3-amino-1,2,4-triazole.

Expression constructs

The pGEX-4T-2-Irga6 construct allowing expression of recombinant GST-Irga6 protein was generated earlier (Uthaiah *et al.*, 2003). The complete coding sequences of mature ROP5 isoforms or GRA7 were amplified by polymerase chain reaction from *T. gondii* strain RHΔ*hxgprt* genomic DNA and ligated into pGAD-C3 or pGBD-C3 (both James *et al.*, 1996). The pGBD-C3-ROP18 construct was generated earlier (Steinfeldt *et al.*, 2010).

Statistics

Significant differences in IRG protein intensities and frequencies at single *T. gondii*-derived intracellular vacuoles were determined using Student's *t*-test under the assumption of unequal variance and with a two-tailed test. The *p*-values are displayed by $p < 0.05$ (single asterisk), $p < 0.01$ (double asterisk) or $p < 0.001$ (triple asterisk) in the respective figures.

Quantification of band intensities in Western blot

Intensities of bands in Fig. 4A were quantified from scanned images using ImageJ software (National Institutes of Health).

Acknowledgements

Jean-Francois Dubremetz provided anti-ROP5 and anti-ROP18 antibodies. John Boothroyd provided *T. gondii* ko strains. Rita Lange contributed to yeast two-hybrid analysis and purification of recombinant protein Irga6. Tobias Lamkemeyer performed MS analysis. Rita Lange and Claudia Poschner provided technical assistance. This work was supported by grants from the Deutsche Forschungsgemeinschaft SFB635, 670, 680, SPP1399 to JCH.

Ethics statement

Animal experimentation: All experiments with mice were conducted under the regulations and protocols for animal experimentation in accordance with the guidelines of the European Commission (Directive 2010/63/EU) and approved by the local government authorities (Bezirksregierung Köln, Germany), LANUV Nordrhein-Westfalen permit no. 44.07.189.

Author contributions

The author(s) have made the following declarations about their contributions: T. H., U. B. M., J. C. H. and T. S. conceived and designed the experiments; T. H., U. B. M., S. K. W. and T.S. performed the experiments; T. H., U. B. M., S. K. W., J. C. H. and T.S. analysed the data; J. C. H. contributed reagents/materials/analysis tools; and T. H., U. B. M., J. C. H. and T. S. wrote the paper.

Conflict of interest

The authors declare that no conflicts of interest exist.

References

Alaganan, A., Fentress, S.J., Tang, K., Wang, Q., and Sibley, L.D. (2014) *Toxoplasma* GRA7 effector increases turnover of immunity-related GTPases and contributes to acute virulence in the mouse. *Proc Natl Acad Sci U S A* **111**, 1126–1131.

Behnke, M.S., Fentress, S.J., Mashayekhi, M., Li, L.X., Taylor, G.A., and Sibley, L.D. (2012) The polymorphic pseudokinase ROP5 controls virulence in *Toxoplasma gondii* by regulating the active kinase ROP18. *PLoS Pathog* **8**, e1002992.

Behnke, M.S., Khan, A., Wootton, J.C., Dubey, J.P., Tang, K., and Sibley, L.D. (2011) Virulence differences in *Toxoplasma* mediated by amplification of a family of polymorphic pseudokinases. *Proc Natl Acad Sci U S A* **108**, 9631–9636.

Bekpen, C., Hunn, J.P., Rohde, C., Parvanova, I., Guethlein, L., Dunn, D.M., *et al*. (2005) The interferon-inducible p47 (IRG) GTPases in vertebrates: loss of the cell autonomous resistance mechanism in the human lineage. *Genome Biol* **6**, R92.

Boehm, U., Guethlein, L., Klamp, T., Ozbek, K., Schaub, A., Futterer, A., *et al*. (1998) Two families of GTPases dominate the complex cellular response to IFN-gamma. *J Immunol* **161**, 6715–6723.

Bonhomme, A., Maine, G.T., Beorchia, A., Burlet, H., Aubert, D., Villena, I., *et al*. (1998) Quantitative immunolocalization of a P29 protein (GRA7), a new antigen of *Toxoplasma gondii*. *J Histochem Cytochem: Official Journal of the Histochemistry Society* **46**, 1411–1422.

Bougdour, A., Durandau, E., Brenier-Pinchart, M.P., Ortet, P., Barakat, M., Kieffer, S., *et al*. (2013) Host cell subversion by *Toxoplasma* GRA16, an exported dense granule protein that targets the host cell nucleus and alters gene expression. *Cell Host Microbe* **13**, 489–500.

Braun, L., Brenier-Pinchart, M.P., Yogavel, M., Curt-Varesano, A., Curt-Bertini, R.L., Hussain, T., *et al*. (2013) A *Toxoplasma* dense granule protein, GRA24, modulates the early immune response to infection by promoting a direct and sustained host p38 MAPK activation. *J Exp Med* **210**, 2071–2086.

Carlow, D.A., Teh, S.J., and Teh, H.S. (1998) Specific antiviral activity demonstrated by TGTP, a member of a new family of interferon-induced GTPases. *J Immunol* **161**, 2348–2355.

Collazo, C.M., Yap, G.S., Sempowski, G.D., Lusby, K.C., Tessarollo, L., Woude, G.F., *et al*. (2001) Inactivation of LRG-47 and IRG-47 reveals a family of interferon gamma-inducible genes with essential, pathogen-specific roles in resistance to infection. *J Exp Med* **194**, 181–188.

Dunn, J.D., Ravindran, S., Kim, S.K., and Boothroyd, J.C. (2008) The *Toxoplasma gondii* dense granule protein GRA7 is phosphorylated upon invasion and forms an unexpected association with the rhoptry proteins ROP2 and ROP4. *Infect Immun* **76**, 5853–5861.

El Hajj, H., Demey, E., Poncet, J., Lebrun, M., Wu, B., Galeotti, N., *et al*. (2006) The ROP2 family of *Toxoplasma gondii* rhoptry proteins: proteomic and genomic characterization and molecular modeling. *Proteomics* **6**, 5773–5784.

Etheridge, R.D., Alaganan, A., Tang, K., Lou, H.J., Turk, B.E., and Sibley, L.D. (2014) The *Toxoplasma* pseudokinase ROP5 forms complexes with ROP18 and ROP17 kinases that synergize to control acute virulence in mice. *Cell Host Microbe* **15**, 537–550.

Fentress, S.J., Behnke, M.S., Dunay, I.R., Mashayekhi, M., Rommereim, L.M., Fox, B.A., *et al*. (2010) Phosphorylation of immunity-related GTPases by a *Toxoplasma gondii*-secreted kinase promotes macrophage survival and virulence. *Cell Host Microbe* **8**, 484–495.

Fentress, S.J., Steinfeldt, T., Howard, J.C., and Sibley, L.D. (2012) The arginine-rich N-terminal domain of ROP18 is necessary for vacuole targeting and virulence of *Toxoplasma gondii*. *Cell Microbiol* **14**, 1921–1933.

Fischer, H.G., Stachelhaus, S., Sahm, M., Meyer, H.E., and Reichmann, G. (1998) GRA7, an excretory 29 kDa *Toxoplasma gondii* dense granule antigen released by infected host cells. *Mol Biochem Parasitol* **91**, 251–262.

Fleckenstein, M.C., Reese, M.L., Konen-Waisman, S., Boothroyd, J.C., Howard, J.C., and Steinfeldt, T. (2012) A *Toxoplasma gondii* pseudokinase inhibits host IRG resistance proteins. *PLoS Biol* **10**, e1001358.

Haldane, J. (1949) Disease and evolution, pp. 68–76.

Haldar, A.K., Saka, H.A., Piro, A.S., Dunn, J.D., Henry, S.C., Taylor, G.A., *et al*. (2013) IRG and GBP host resistance factors target aberrant, 'non-self' vacuoles characterized by the missing of 'self' IRGM proteins. *PLoS Pathog* **9**, e1003414.

Hunn, J.P., Koenen-Waisman, S., Papic, N., Schroeder, N., Pawlowski, N., Lange, R., *et al*. (2008) Regulatory interactions between IRG resistance GTPases in the cellular response to *Toxoplasma gondii*. *Embo J* **27**, 2495–2509.

Hunter, C.A., and Sibley, L.D. (2012) Modulation of innate immunity by *Toxoplasma gondii* virulence effectors. *Nat Rev Microbiol* **10**, 766–778.

James, P., Halladay, J., and Craig, E.A. (1996) Genomic libraries and a host strain designed for highly efficient two-hybrid selection in yeast. *Genetics* **144**, 1425–1436.

Khaminets, A., Hunn, J.P., Konen-Waisman, S., Zhao, Y.O., Preukschat, D., Coers, J., *et al*. (2010) Coordinated loading of IRG resistance GTPases on to the *Toxoplasma gondii* parasitophorous vacuole. *Cell Microbiol* **12**, 939–961.

Leriche, M.A., and Dubremetz, J.F. (1991) Characterization of the protein contents of rhoptries and dense granules of *Toxoplasma gondii* tachyzoites by subcellular fractionation and monoclonal antibodies. *Mol Biochem Parasitol* **45**, 249–259.

Liesenfeld, O., Parvanova, I., Zerrahn, J., Han, S.J., Heinrich, F., Munoz, M., *et al*. (2011) The IFN-gamma-inducible GTPase, Irga6, protects mice against *Toxoplasma gondii* but not against *Plasmodium berghei* and some other intracellular pathogens. *PLoS One* **6**, e20568.

Lilue, J., Muller, U.B., Steinfeldt, T., and Howard, J.C. (2013) Reciprocal virulence and resistance polymorphism in the relationship between *Toxoplasma gondii* and the house mouse. *eLife* **2**, e01298.

Lim, D., Gold, D.A., Julien, L., Rosowski, E.E., Niedelman, W., Yaffe, M.B., and Saeij, J.P. (2013) Structure of the *Toxoplasma gondii* ROP18 kinase domain reveals a second ligand binding pocket required for acute virulence. *J Biol Chem* **288**, 34968–34980.

Ling, Y.M., Shaw, M.H., Ayala, C., Coppens, I., Taylor, G.A., Ferguson, D.J., and Yap, G.S. (2006) Vacuolar and plasma membrane stripping and autophagic elimination of *Toxoplasma gondii* in primed effector macrophages. *J Exp Med* **203**, 2063–2071.

Luo, Q., Upadhya, R., Zhang, H., Madrid-Aliste, C., Nieves, E., Kim, K., *et al*. (2011) Analysis of the glycoproteome of *Toxoplasma gondii* using lectin affinity chromatography and tandem mass spectrometry. *Microbes Infect Institut Pasteur* **13**, 1199–1210.

Martens, S., and Howard, J. (2006) The interferon-inducible GTPases. *Annu Rev Cell Dev Biol* **22**, 559–589.

Martens, S., Parvanova, I., Zerrahn, J., Griffiths, G., Schell, G., Reichmann, G., and Howard, J.C. (2005) Disruption of *Toxoplasma gondii* parasitophorous vacuoles by the mouse p47-resistance GTPases. *PLoS Pathog* **1**, e24.

Martens, S., Sabel, K., Lange, R., Uthaiah, R., Wolf, E., and Howard, J.C. (2004) Mechanisms regulating the positioning of mouse p47 resistance GTPases LRG-47 and IIGP1 on

cellular membranes: retargeting to plasma membrane induced by phagocytosis. *J Immunol* **173**, 2594–2606.
Niedelman, W., Gold, D.A., Rosowski, E.E., Sprokholt, J.K., Lim, D., Farid Arenas, A., *et al.* (2012) The rhoptry proteins ROP18 and ROP5 mediate *Toxoplasma gondii* evasion of the murine, but not the human, interferon-gamma response. *PLoS Pathog* **8**, e1002784.
Papic, N., Hunn, J.P., Pawlowski, N., Zerrahn, J., and Howard, J.C. (2008) Inactive and active states of the interferon-inducible resistance GTPase, Irga6, *in vivo*. *J Biol Chem* **283**, 32143–32151.
Reese, M.L., and Boothroyd, J.C. (2011) A conserved non-canonical motif in the pseudoactive site of the ROP5 pseudokinase domain mediates its effect on *Toxoplasma* virulence. *J Biol Chem* **286**, 29366–29375.
Reese, M.L., Shah, N., and Boothroyd, J.C. (2014) The *Toxoplasma* pseudokinase ROP5 is an allosteric inhibitor of the immunity-related GTPases. *J Biol Chem* **289**, 27849–27858.
Reese, M.L., Zeiner, G.M., Saeij, J.P., Boothroyd, J.C., and Boyle, J.P. (2011) Polymorphic family of injected pseudokinases is paramount in *Toxoplasma* virulence. *Proc Natl Acad Sci U S A* **108**, 9625–9630.
Saeij, J.P., Boyle, J.P., Coller, S., Taylor, S., Sibley, L.D., Brooke-Powell, E.T., *et al.* (2006) Polymorphic secreted kinases are key virulence factors in toxoplasmosis. *Science* **314**, 1780–1783.
Saeij, J.P., Coller, S., Boyle, J.P., Jerome, M.E., White, M.W., and Boothroyd, J.C. (2007) Toxoplasma co-opts host gene expression by injection of a polymorphic kinase homologue. *Nature* **445**, 324–327.
Steinfeldt, T., Konen-Waisman, S., Tong, L., Pawlowski, N., Lamkemeyer, T., Sibley, L.D., *et al.* (2010) Phosphorylation of mouse immunity-related GTPase (IRG) resistance proteins is an evasion strategy for virulent *Toxoplasma gondii*. *PLoS Biol* **8**, e1000576.
Taylor, G.A. (2007) IRG proteins: key mediators of interferon-regulated host resistance to intracellular pathogens. *Cell Microbiol* **9**, 1099–1107.
Taylor, G.A., Collazo, C.M., Yap, G.S., Nguyen, K., Gregorio, T.A., Taylor, L.S., *et al.* (2000) Pathogen-specific loss of host resistance in mice lacking the IFN-gamma-inducible gene IGTP. *Proc Natl Acad Sci U S A* **97**, 751–755.
Taylor, G.A., Feng, C.G., and Sher, A. (2007) Control of IFN-gamma-mediated host resistance to intracellular pathogens by immunity-related GTPases (p47 GTPases). *Microbes Infect Institut Pasteur* **9**, 1644–1651.
Taylor, S., Barragan, A., Su, C., Fux, B., Fentress, S.J., Tang, K., *et al.* (2006) A secreted serine-threonine kinase determines virulence in the eukaryotic pathogen *Toxoplasma gondii*. *Science* **314**, 1776–1780.
Treeck, M., Sanders, J.L., Elias, J.E., and Boothroyd, J.C. (2011) The phosphoproteomes of *Plasmodium falciparum* and *Toxoplasma gondii* reveal unusual adaptations within and beyond the parasites' boundaries. *Cell Host Microbe* **10**, 410–419.
Uthaiah, R.C., Praefcke, G.J., Howard, J.C., and Herrmann, C. (2003) IIGP1, an interferon-gamma-inducible 47-kDa GTPase of the mouse, showing cooperative enzymatic activity and GTP-dependent multimerization. *J Biol Chem* **278**, 29336–29343.
Zhao, Y., Ferguson, D.J., Wilson, D.C., Howard, J.C., Sibley, L.D., and Yap, G.S. (2009a) Virulent *Toxoplasma gondii* evade immunity-related GTPase-mediated parasite vacuole disruption within primed macrophages. *J Immunol* **182**, 3775–3781.
Zhao, Y.O., Khaminets, A., Hunn, J.P., and Howard, J.C. (2009b) Disruption of the *Toxoplasma gondii* parasitophorous vacuole by IFNgamma-inducible immunity-related GTPases (IRG proteins) triggers necrotic cell death. *PLoS Pathog* **5**, e1000288.
Zhao, Y.O., Rohde, C., Lilue, J.T., Konen-Waisman, S., Khaminets, A., Hunn, J.P., and Howard, J.C. (2009c) *Toxoplasma gondii* and the immunity-related GTPase (IRG) resistance system in mice: a review. *Mem Inst Oswaldo Cruz* **104**, 234–240.

Supporting information

Additional Supporting Information may be found in the online version of this article at the publisher's web-site:

Table S1. *T. gondii* proteins in complex with GST-Irga6

Fig. S1. Determination of protein levels for *T. gondii* strains. Western blot of *T. gondii* RHΔ*hxgprt*, RHΔ*gra7* and RHΔ*rop18* tachyzoite detergent lysates. Relative levels of ROP18 (middle left panel), ROP5 (middle right panel) and GRA7 (lower panels) were determined using specific antibodies and calnexin (upper panels) served as loading control.

Fig. S2. Vacuolar IRG protein loading is increased in the absence of GRA7. IFNγ-induced MEFs (200 U ml^{-1}) were infected for 2 h with *T. gondii* RHΔ*hxgprt* or RHΔ*gra7*, and individual IRG protein positive vacuoles identified with mouse monoclonal antibody B34 (Irgb6) or 940/6 (Irgb10) and 2078 (Irgd) rabbit antisera. (A–C) Upper panels: phase contrast images. Lower panels: fluorescent images of vacuoles (white arrows) from RHΔ*hxgprt* or RHΔ*gra7* loaded with Irgb6 (A, green), Irgb10 (B, green) and Irgd (C, green). Nuclei stained with 4′,6-diamidino-2-phenylindole (blue). (D) The percentage of IRG protein positive vacuoles was evaluated by visual inspection of coded slides. The results of two independent experiments are shown (100 vacuoles counted).

Fig. S3. Determination of *T. gondii* RHΔ*hxgprt* median lethal dose in CIM mice. CIM mice were infected by intraperitoneal injection of indicated numbers of *T. gondii* RHΔ*hxgprt* strain tachyzoites, and survival was monitored for 80 days. NMRI mice infected with 1000 *T. gondii* tachyzoites served as control to confirm RHΔ*hxgprt* strain virulence.

Fig. S4. IRG protein levels in C57BL/6 wt and *Irga6* ko MEFs. Western blot of detergent lysates from C57BL/6 wt and *Irga6* ko MEFs stimulated for 24 h with 200 U ml^{-1} of IFNγ or left untreated. Monoclonal antibodies 10E7 (Irga6, lower left panel) and B34 (Irgb6, lower middle panel) or rabbit antiserum 940/6 (Irgb10, lower right panel) were

used to determine relative IRG protein levels. The upper band of a doublet in the case of Irgb10 could represent phosphorylated protein detected in non-infected cells (Steinfeldt *et al*., 2010). Calnexin (upper panels) served as loading control.

Fig. S5. Frequencies of IRG positive vacuoles in infected wt and *Irga6* ko MEFs. After infection of IFNγ-induced (200 U ml^{-1}) wt or *Irga6* ko MEFs for 2 h with *T. gondii*, RHΔ*hxgprt*, RHΔ*gra7*, RHΔ*rop18* or RHΔ*rop5* individual IRG protein positive vacuoles were analysed. The increase in numbers of Irgb6 and Irgb10 positive RHΔ*gra7*-derived and RHΔ*rop18*-derived vacuoles in wt MEFs is strongly inhibited in *Irga6* ko MEFs. The number of Irgb6 and Irgb10 positive RHΔ*hxgprt*-derived vacuoles is also slightly reduced in *Irga6* ko compared with wt MEFs, but no significant difference was observed for RHΔ*rop5* when comparing both cell types. The results of three independent experiments are shown (150 vacuoles counted).

